Research Article

Qingsong Wang* and Ming Gao

Performance evaluation of common-aperture visible and long-wave infrared imaging system based on a comprehensive resolution

https://doi.org/10.1515/phys-2022-0200
received April 01, 2022; accepted September 15, 2022

Abstract: In this article, a new method based on a comprehensive resolution is proposed to evaluate the performance of a common-aperture visible and long-wave infrared (LWIR) imaging system. The influence of the comprehensive resolution on target recognition range is analyzed. Under the condition of common-aperture and a combination of four comprehensive resolutions, the main factors affecting the ratio of target recognition range between the visible imaging system and the LWIR imaging system are discussed. Combined with the constraints of the optical system and the detector, the impact of the comprehensive resolution on the target recognition range is analyzed. The ratio of the target recognition range of the two imaging systems is modeled using the comprehensive resolution of the visible imaging system. The experimental system is built and the experimental results are acquired. The predictive results and experimental results show that when the comprehensive resolution of the visible light imaging system increases, the target recognition ranges of the visible light imaging system and the LWIR imaging system increase, as well as the ratio of the target recognition ranges of the two systems increases.

Keywords: comprehensive resolution, common-aperture, dual-band imaging system, target recognition range

1 Introduction

Dual-band imaging system used in the target acquisition missions in the military field usually consists of two single-aperture single-band imaging systems. However, the common-aperture dual-band imaging system is more attractive with the continuous improvement of the performance, weight, volume, and structure of the imaging system in modern warfare [1,2]. Common-aperture dual-band imaging system shares part or all of the optical systems and uses the same display but detectors in different wavelength bands.

When comparing visible imaging with long-wave infrared (LWIR) imaging, the former has the advantages of high resolution and the disadvantage of being easily affected by ambient light, while the latter has the advantages of strong penetrating capability and independent of ambient light, and the disadvantage of smaller resolution [3,4]. In recent years, research articles on common-aperture visible and LWIR imaging systems (VaLWIRIS) have appeared continuously [5–7].

The method of evaluation of common-aperture VaLWIRIS performance is usually the same as that of single-channel single-band imaging systems. The U.S. Army uses the Night Vision Integrated Performance Model (NVIPM) based on the Targeting Task Performance (TTP) metric to evaluate the imaging system performance [8,9]. The NVIPM is a very complex evaluation model. At the same time, the influence of the structural characteristics of a common-aperture imaging system on the system performance needs to be considered in order to make a trade-off between visible imaging system performance and LWIR imaging system performance. In this article, a method for evaluating the performance of common-aperture VaLWIRIS is proposed by combining the comprehensive resolution and the structural characteristics of the common-aperture imaging system.

2 Evaluation of imaging system performance

An imaging system includes optical system, detector array, signal processing, and display. The target acquisition

* **Corresponding author: Qingsong Wang,** School of Optoelectronic Engineering, Xi'an Technological University, Xi'an, 710021, China, e-mail: wangqingsong@xatu.edu.cn
Ming Gao: School of Optoelectronic Engineering, Xi'an Technological University, Xi'an, 710021, China

process based on the imaging system is shown in Figure 1.

Target and background of a scene are imaged on detectors by an optical system. The detectors then convert the light intensity into electrical signals, which are processed by electronic system and passed to the display to reconstruct the image. The observer acquires (*e.g.*, detects, recognizes, and identifies) the target by viewing the image on the display.

The target acquisition range is one of the most important performance parameters of the imaging system, which is evaluated by a model related to many parameters. These parameters describe imaging system, target characteristics, atmospheric conditions, display, and observer. NVIPM based on the TTP metric is an integrated model that predicts the target acquisition range. The TTP metric is defined as follows [8,9]:

$$M_{\mathrm{TTP}} = \int_{u_{\mathrm{L}}}^{u_{\mathrm{H}}} \sqrt{\frac{C_{\mathrm{T}}}{C_{\mathrm{S}}(u)}}\,\mathrm{d}u = \int_{u_{\mathrm{L}}}^{u_{\mathrm{H}}} \sqrt{\frac{C_{\mathrm{T}}}{\frac{C_{\mathrm{E}}(u)}{M_{\mathrm{S}}(u)}\left(1+\frac{\alpha^2 N^2(u)}{L^2}\right)^{1/2}}}\,\mathrm{d}u, \tag{1}$$

where M_{TTP} is the TTP metric (cycles mrad^{-1}); u is the spatial frequency (cycles mrad^{-1}); $C_{\mathrm{S}}(u)$ is the contrast thresholds function (CTF) for the imaging systems; $C_{\mathrm{E}}(u)$ is the CTF for the eyes; $M_{\mathrm{S}}(u)$ is the modulation transfer function (MTF) of the system; $N(u)$ is the RMS noise of the display; α is the empirical constant; L is the luminance of the display (cd m^{-2}); C_{T} is the contrast of the target on the display; u_{H} and u_{L} are the intersection of C_{T} and $C_{\mathrm{S}}(u)$ (cycles mrad^{-1}). Details of $C_{\mathrm{S}}(u)$, $C_{\mathrm{E}}(u)$, $M_{\mathrm{S}}(u)$, and $N(u)$ are shown in refs. [8,9].

If giving the target contrast, the characteristic dimension, the target acquisition task and the number of cycles on the target, the target acquisition range can be obtained by

$$R = \frac{W_{\mathrm{T}}}{V} M_{\mathrm{TTP}}, \tag{2}$$

where R is the target acquisition range (km), W_{T} is the characteristic dimension of the target (m), and V is the number of cycles on the target.

It can be known from Eq. (1) that Eq. (2) is a very complex performance model. When the atmospheric transmittance is 1, the observer viewing distance is fixed and the imaging system does not have any noise; Eq. (2) is simplified [10,11] as

$$R \approx \frac{W_{\mathrm{T}}}{V} K V_{\mathrm{FOM}} \frac{D}{\lambda}, \tag{3}$$

where D is the diameter of the clear aperture (mm), λ is the wavelength (μm), and K is the calibration coefficient, which is related to display luminance and target contrast on the display; V_{FOM} is the figure of merit, which is expressed as

$$V_{\mathrm{FOM}} \approx \int_0^{u_{\mathrm{n}}} \sqrt{\frac{M_{\mathrm{O}}(u) M_{\mathrm{D}}(u) M_{\mathrm{FP}}(u)}{C_{\mathrm{E}}(u)}}\,\mathrm{d}u, \tag{4}$$

where u_{n} is the Nyquist frequency (cycles mrad^{-1}); $M_{\mathrm{O}}(u)$, $M_{\mathrm{D}}(u)$, and $M_{\mathrm{FP}}(u)$ are the MTF of optical system, detector, and flat panel display, respectively.

The comprehensive resolution [12,13] is defined as

$$Q = \frac{u_{\mathrm{D}}}{u_{\mathrm{O}}} = \frac{f'\lambda}{Dd} = \frac{F\lambda}{d}, \tag{5}$$

where Q is the comprehensive resolution, u_{O} is the cutoff frequencies of the optical system (cycles mrad^{-1}), u_{D} is the cutoff frequencies of the detector (cycles mrad^{-1}); f' is the focal length of the optical system (mm); d is the detector size (μm); and F is F-number.

For target recognition task, a curve fit valid up to $Q = 4$ is [10,11]

$$V_{\mathrm{FOM\_R}} \approx b_6 Q^6 + b_5 Q^5 + b_4 Q^4 + b_3 Q^3 + b_2 Q^2 + b_1 Q, \tag{6}$$

where $V_{\mathrm{FOM\_R}}$ is the figure of merit of recognition; $b_6 = -0.00247$; $b_5 = 0.0261$; $b_4 = -0.0901$; $b_3 = 0.1098$; $b_2 = -0.1582$; $b_1 = 0.7402$.

The polynomial relationship between $V_{\mathrm{FOM\_R}}$ and Q is shown in Figure 2. According to the definition of Q and

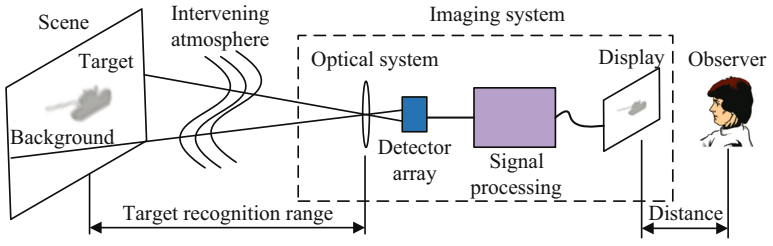

Figure 1: Target acquisition process based on the imaging system.

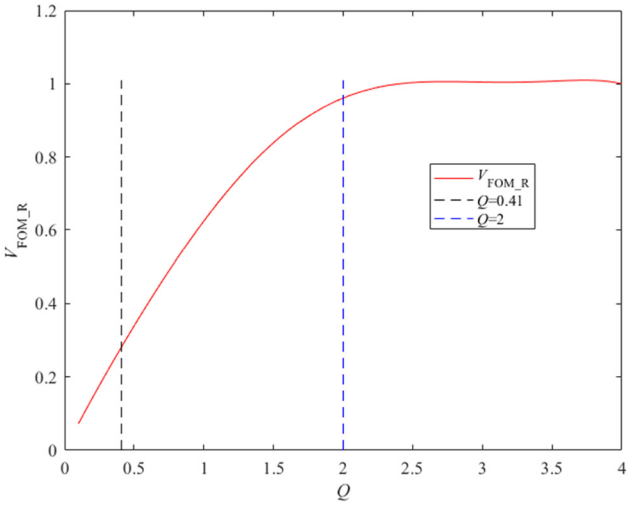

Figure 2: Polynomial relationship between V_{FOM_R} and Q.

the changing trend of V_{FOM_R}, the curve can be divided into three regions: the detector-limited region for $Q \le 0.41$, the transition region for $0.41 < Q < 2$, and the optics-limited region for $2 \le Q \le 4$.

When $Q \le 0.41$, the detector cutoff frequency is less than or equal to the optical cutoff frequency, the imaging system performance is limited by the detector; the first five terms of Eq. (6) become very small, so that Eq. (3) can be approximated as

$$R_{Rec} \approx b_1 \frac{W_T}{V} K \frac{f'}{d} = b_1 \frac{W_T}{V} K \frac{1}{\alpha_D}, \tag{7}$$

where R_{Rec} is the target recognition range (km); α_D is the detector angular subtenses (mrad).

Eq. (7) shows that the target recognition range is independent of wavelength, proportional to focal length, and inversely proportional to the detector size and angular subtenses.

When $2 \le Q \le 4$, the detector cutoff frequency is between 2 times and 4 times of the optical cutoff frequency, the imaging system performance is optics-limited. It can be found from Figure 1 that V_{FOM_R} plateaus to a fixed value named as $V_{FOM\_R\_M}$ which is approximately 1. Eq. (3) can be approximated as

$$R_{Rec} \approx V_{FOM\_R\_M} \frac{W_T}{V} K \frac{D}{\lambda} \approx \frac{W_T}{V} K \frac{D}{\lambda}. \tag{8}$$

Eq. (8) shows that the target recognition range of the imaging system is proportional to the diameter of clear aperture and inversely proportional to wavelength.

When the value of Q changes from 0.41 to 2, the system performance is in the transition region from detector-limited to optics-limited. The target recognition range of the imaging system is calculated by Eq. (3).

3 Performance of common-aperture VaLWIRIS

According to the value of Q, common-aperture VaLWIRIS can be combined in nine cases as shown in Table 1. Due to space limitations, only four cases are discussed here. They are cases No. 1, 3, 7, and 9.

3.1 Detector-limited visible imaging system and LWIR imaging system

When the performance of the visible imaging system and the LWIR imaging system are both detector-limited, it can be known from Eq. (7) that the ratio of the target recognition ranges between visible imaging system and LWIR imaging system is

$$R_{Rat} = \frac{R_V}{R_{LWIR}} \approx \frac{b_1 \frac{W_T}{V} \sqrt{C_T} \frac{f'}{d_V}}{b_1 \frac{W_T}{V} \sqrt{C_T} \frac{f'}{d_{LWIR}}} = \frac{d_{LWIR}}{d_V}, \tag{9}$$

where R_{Rat} is the ratio of the target recognition ranges; R_V and R_{LWIR} are the target recognition ranges in km of the visible imaging system and LWIR, respectively; d_V and d_{LWIR} are the detector sizes in μm of the visible imaging system and LWIR imaging system, respectively.

Eq. (9) shows that when the VaLWIRIS use common-aperture optical system with the same focal length if the performances of the visible imaging system and the LWIR imaging system are both detector-limited, the ratio of the

Table 1: Nine combinations of common-aperture VaLWIRIS

Serial number	Visible imaging system	LWIR imaging system
1	Detector-limited	Detector-limited
2	Detector-limited	Transition region
3	Detector-limited	Optics-limited
4	Transition region	Detector-limited
5	Transition region	Transition region
6	Transition region	Optics-limited
7	Optics-limited	Detector-limited
8	Optics-limited	Transition region
9	Optics-limited	Optics-limited

two target recognition ranges is the ratio of the LWIR detector size to the visible detector size. Usually, d_{LWIR} is larger than d_{V}; therefore, R_{ra} is larger than 1.

3.2 Optics-limited visible imaging system and detector-limited LWIR imaging system

When the visible imaging system is optics-limited and the LWIR imaging system is detector-limited, it can be obtained from Eqs. (7) and (8) that the ratio of target recognition ranges between visible imaging system and LWIR imaging system is

$$R_{\mathrm{Rat}} = \frac{R_{\mathrm{V}}}{R_{\mathrm{LWIR}}} \approx \frac{K\frac{W_{\mathrm{T}}}{V}\frac{D}{\lambda_{\mathrm{V}}}}{Kb_1\frac{W_{\mathrm{T}}}{V}\frac{f'}{d_{\mathrm{LWIR}}}} \approx \frac{d_{\mathrm{LWIR}}}{Fb_1\lambda_{\mathrm{V}}}, \tag{10}$$

where, λ_{V} is the visible wavelength (μm).

Eq. (10) shows that the ratio is proportional to the size of the LWIR detector and inversely proportional to the optical system F-number and the visible wavelength. When the values of λ_{V}, F, b_1, and d_{LWIR} are 0.5 μm, 4, 0.7402, and 17 μm, respectively, R_{ra} is 11.48. When F decreases, the target recognition range of the visible imaging system is much larger than that of the LWIR imaging system.

3.3 Detector-limited visible imaging system and optics-limited LWIR imaging system

When the visible imaging system is detector-limited and the LWIR imaging system is optics-limited, it can be obtained from Eqs. (7) and (8) that the ratio of target recognition ranges between visible imaging system and LWIR imaging system is

$$R_{\mathrm{Rat}} = \frac{R_{\mathrm{V}}}{R_{\mathrm{LWIR}}} \approx \frac{Kb_1\frac{W_{\mathrm{T}}}{V}\frac{f'}{d_{\mathrm{V}}}}{K\frac{W_{\mathrm{T}}}{V}\frac{D}{\lambda_{\mathrm{LWIR}}}} \approx b_1F\frac{\lambda_{\mathrm{LWIR}}}{d_{\mathrm{V}}}, \tag{11}$$

where λ_{LWIR} is the LWIR wavelength (μm).

Eq. (11) shows that the ratio is proportional to the LWIR wavelength and the optical system F-number, and inversely proportional to the size of the visible detector. The ratio is larger than 1 when F, d_{V}, and λ_{LWIR} take common values.

3.4 Optics-limited visible imaging system and LWIR imaging system

In this situation, the ratio of the target recognition ranges between visible imaging system and LWIR imaging system can be obtained by Eq. (8)

$$R_{\mathrm{Rat}} = \frac{R_{\mathrm{V}}}{R_{\mathrm{LWIR}}} \approx \frac{K\frac{W_{\mathrm{T}}}{V}\frac{D}{\lambda_{\mathrm{V}}}}{K\frac{W_{\mathrm{T}}}{V}\frac{D}{\lambda_{\mathrm{LWIR}}}} = \frac{\lambda_{\mathrm{LWIR}}}{\lambda_{\mathrm{V}}}. \tag{12}$$

It can be known from Eq. (12) that the ratio is proportional to the LWIR wavelength and inversely proportional to the visible wavelength. R_{ra} is larger than 1 because λ_{LWIR} is larger than λ_{V}.

4 Influence of the comprehensive resolution of visible imaging system on the target recognition range

For ease of discussion, let the wavelengths of visible and LWIR be 0.5 μm and 10 μm, respectively. The detector size of optics-limited visible imaging system is

$$d_{\mathrm{V\_O}} \le \frac{1}{2}F\lambda_{\mathrm{V}}. \tag{13}$$

The detector size of the detector-limited visible imaging system is

$$d_{\mathrm{V\_D}} \ge \frac{1}{0.41}F\lambda_{\mathrm{V}}. \tag{14}$$

The detector size of optics-limited LWIR imaging system is

$$d_{\mathrm{LWIR\_O}} \le \frac{1}{2}F\lambda_{\mathrm{LWIR}}. \tag{15}$$

The detector size of the detector-limited LWIR imaging system is

$$d_{\mathrm{LWIR\_D}} \ge \frac{1}{0.41}F\lambda_{\mathrm{LWIR}}. \tag{16}$$

It can be seen from Eq. (9) that the imaging system has the maximum target recognition range when $Q \ge 2$. When F = 1–4, the visible detector size is required to be between 0.25 and 1 μm, and the LWIR detector size is required to be between 5 and 20 μm. For the visible

detectors, the actual size that can be selected is generally larger than 1 μm. Therefore, the visible imaging system usually is detector-limited. For the LWIR detectors, its actual size that can be selected is between 10 and 35 μm; hence, the LWIR imaging system may be detector-limited, optics-limited, or transitional.

4.1 Influence of focal length and clear aperture on comprehensive resolution

For ease of discussion, let the detector sizes of visible imaging system and LWIR imaging system be 5 μm and 17 μm, respectively. According to Eq. (5), the comprehensive resolution is plotted as a function of focal length with the clear aperture as a parameter in Figure 3. It shows that the larger the focal length, the larger the comprehensive resolution; the smaller the clear aperture, the larger the comprehensive resolution. The comprehensive resolution of the visible imaging system is smaller than that of LWIR imaging system. The comprehensive resolution of the visible imaging system is less than 0.41, indicating that the performance of the visible imaging system is detector-limited. The comprehensive resolution of LWIR imaging system is between 1 and 2.5, indicating that the LWIR imaging system is transitional or optics-limited.

4.2 Influence of focal length and clear aperture on target recognition range

According to Eq. (3), the target recognition range is plotted as a function of focal length with the clear aperture as a parameter in Figure 4. It shows that the larger the focal length, the larger the target recognition range; the larger the clear aperture, the smaller the target recognition range. Under the conditions of the same focal length and clear aperture, the target recognition range of visible imaging system is much larger than that of the LWIR imaging system.

4.3 Influence of comprehensive resolution on target recognition range

According to Eqs. (3)–(6), the target recognition range is plotted as a function of comprehensive resolution with the clear aperture as a parameter in Figure 5. It shows that when the common-aperture method is adopted, both the comprehensive resolution and target recognition range of the two systems are different. When the diameter of the clear aperture is 50 mm, the larger the comprehensive resolution, the larger the target recognition range of LWIR imaging system. But when the comprehensive resolution is larger than 2, the target recognition range of LWIR imaging system is almost kept constant. For visible

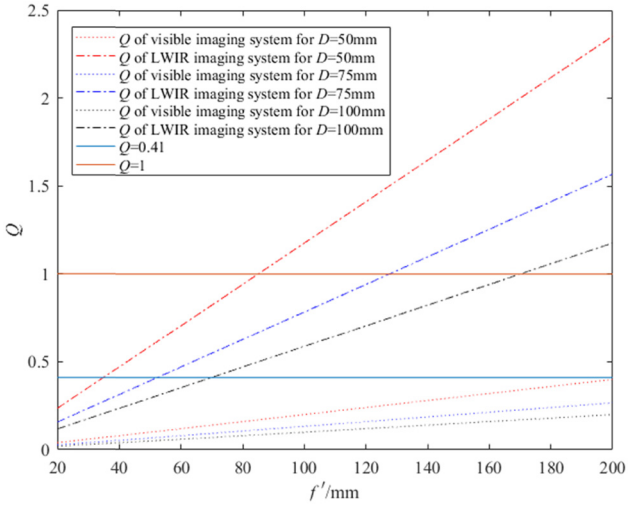

Figure 3: Comprehensive resolution as a function of f' with the clear aperture as a variable.

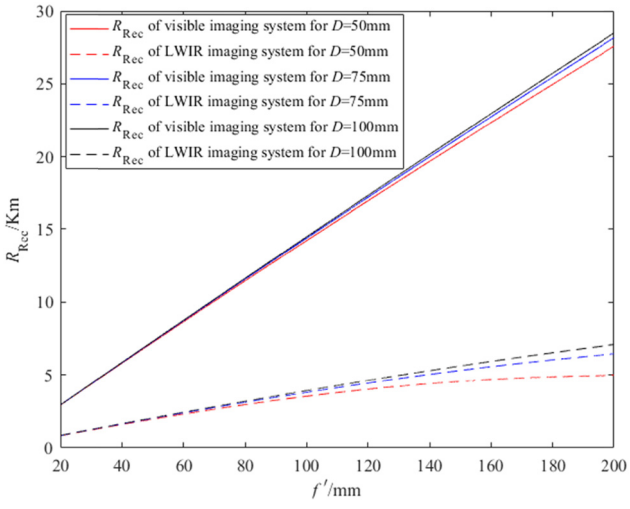

Figure 4: Target recognition range as a function of f' with the clear aperture as a variable.

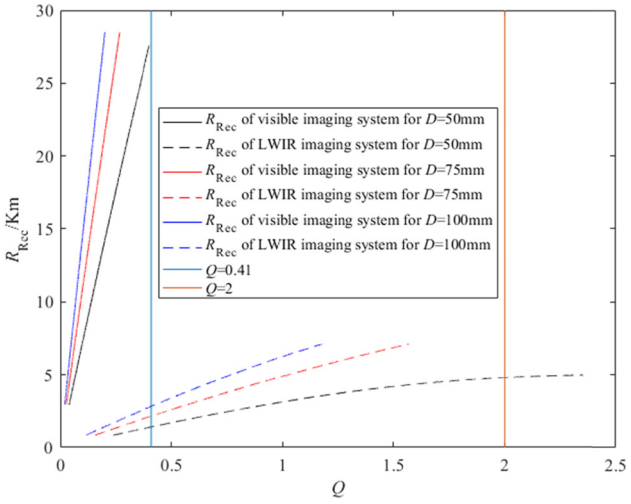

Figure 5: Target recognition range as a function of Q with the clear aperture as a variable.

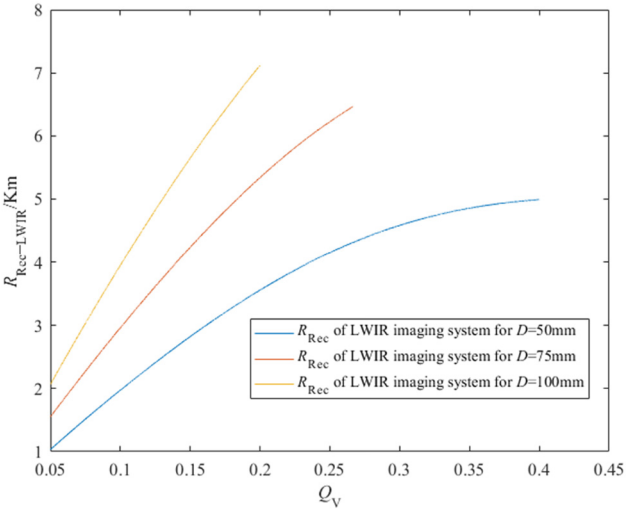

Figure 6: Target recognition range of LWIR imaging system as a function of Q_V with the clear aperture as a variable.

imaging system, the larger the comprehensive resolution, the larger the target recognition range.

4.4 Influence of the comprehensive resolution on the target recognition range ratio

For common-aperture VaLWIRIS, the expression for calculating the target recognition range of LWIR imaging system using the comprehensive resolution of the visible imaging system is

$$\begin{aligned} R_{\text{Rec\_LWIR}} &\approx \frac{W_T}{V} K V_{\text{FOM\_R\_LWIR}} \frac{D}{\lambda_{\text{LWIR}}} \\ &= \frac{D}{\lambda_{\text{LWIR}}} \frac{W_T}{V} K V_{\text{FOM\_R}}(G Q_V), \end{aligned} \tag{17}$$

where $R_{\text{Rec\_LWIR}}$ is the target recognition range of the LWIR imaging system and G is given by

$$G = \frac{\lambda_{\text{LWIR}} d_V}{\lambda_V d_{\text{LWIR}}}. \tag{18}$$

When Q_V varies between 0.1 and 0.41, the relationship between the target recognition range of the LWIR imaging system and the comprehensive resolution of the visible imaging system under different clear apertures is shown in Figure 6.

The relationship between the ratio of the target recognition ranges of the two systems and the comprehensive resolution of the visible imaging system is

$$\begin{aligned} R_{\text{Rat}} &= \frac{R_V}{R_{\text{LWIR}}} \approx \frac{b_1}{V_{\text{FOM\_R\_LWIR}}} \left(\frac{F}{d}\right)_V \\ &= K_\lambda b_1 \frac{1}{V_{\text{FOM\_R\_LWIR}}} Q_V, \end{aligned} \tag{19}$$

where R_{Rat} is the ratio of target recognition ranges of the two systems; $K_\lambda = \lambda_{\text{LWIR}}/\lambda_V$.

Eq. (19) shows that the ratio of the target recognition ranges of the two systems is proportional to the comprehensive resolution of the visible imaging system and inversely proportional to the factor of merit of the LWIR imaging system. Figure 7 shows the relationship between

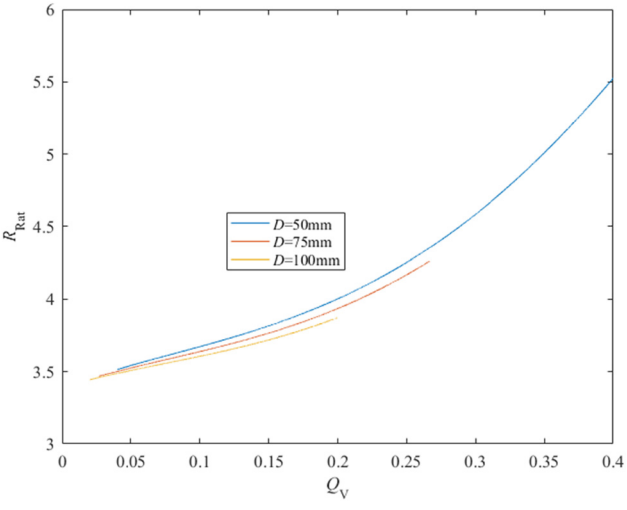

Figure 7: Target recognition range ratio as a function of Q_V with the clear aperture as a variable.

the ratio of the target recognition ranges of the two systems and the comprehensive resolution of the visible imaging system. It can be seen that as the comprehensive resolution of the visible imaging system increases, the ratio of the target recognition ranges of the two systems increases.

Table 2: Main parameters of the cameras

Camera	Pixel pitch (μm)	Average wavelength (μm)
Gobi-640-Gige	17	11
X8500sc-SLS	12	9
MER-20-20GM	4.4	0.55
Aca640-90gm	7.4	0.55

5 Experiments

5.1 Experimental system

A common-aperture VaLWIRIS is built in the laboratory. The relationship between the target recognition range and the comprehensive resolution is verified. The schematic diagram of the experiment is shown in Figure 8. The whole experimental system consists of visible source, visible target, blackbody, LWIR target, off-axis reflective collimator, common-aperture visible and LWIR optical system, LWIR camera, visible camera, computer, display, and observer.

The focal length of the optical system is 50 mm, the diameter of the clear aperture is 35.7 mm, and the *F*-number is 1.4. The main parameters of the cameras are shown in Table 2.

5.2 Results and discussion

5.2.1 Target recognition range

The predictive results and the average results of multiple experiments for the target recognition ranges of common-aperture VaLWIRISs are shown in Table 3.

The comprehensive resolution of both the X8500sc-SLS and the Gobi-640-Gige is between 0.41 and 2. The comprehensive resolution of the Gobi-640-Gige is smaller than that of the X8500sc-SLS. According to Eq. (3), the predictive target recognition range of Gobi-640-Gige is smaller than that of X8500sc-SLS. The same goes for the experimental results.

The comprehensive resolution of both the MER-20-20GM and the Aca640-90gm is less than 0.41. The comprehensive resolution of the MER-20-20GM is smaller than that of the Aca640-90gm. According to Eq. (7), the predictive target recognition range of MER-20-20GM is larger than that of Aca640-90gm. The same goes for the experimental results.

Table 3 shows that there is a certain error between the predictive target recognition range and the experimental target recognition range. This is because Eqs. (3) and (7) are obtained under conditions that are slightly changed during the experiment. Nevertheless, the trends in the predictive results are consistent with those in the experimental results. According to the predictive results, the influence of the parameters of the common-aperture optical system on the target recognition range of the two systems can be analyzed.

5.2.2 Target recognition range ratio

The ratio of the target recognition ranges of visible imaging systems to that of LWIR imaging systems is shown in Table 4.

The predictive ratio of the target recognition range of MER-20-20GM to that of Gobi-640-Gige is larger than the predictive ratio of the target recognition range of MER-20-20GM to that of X8500sc-SLS because the comprehensive

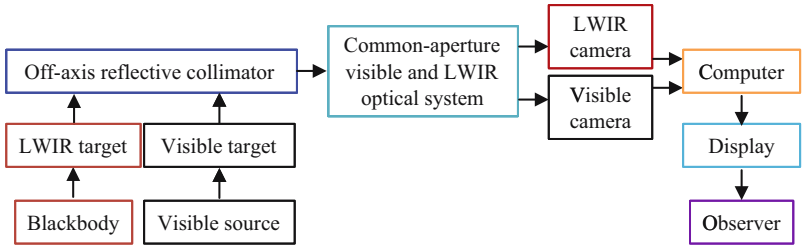

Figure 8: Schematic diagram of the target recognition range experiment.

Table 3: Target recognition ranges of visible imaging systems and LWIR imaging systems

Imaging system	*Q*	FOM	Target recognition range (m)		Error (%)
			Predictive	Experimental	
Gobi-640-Gige	0.906	0.57	1.87	1.90	1.5
X8500sc-SLS	1.05	0.65	2.57	2.53	−1.6
MER-20-20GM	0.175	0.12	7.93	7.72	−5.3
Aca640-90gm	0.35	0.07	4.89	4.7	−4.2

Table 4: Ratios of the target recognition ranges between visible imaging systems and LWIR imaging systems

Visible imaging system	LWIR imaging system	Target recognition range ratio	
		Predictive	Experimental
MER-20-20GM	Gobi-640-Gige	4.35	4.06
MER-20-20GM	X8500sc-SLS	3.15	3.05
Aca640-90gm	Gobi-640-Gige	2.6	2.47
Aca640-90gm	X8500sc-SLS	1.89	1.86

resolution of Gobi-640-Gige is smaller than that of X8500sc-SLS. The same goes for the experimental results. Aca640-90gm also has the same phenomenon as MER-20-20GM. For the same visible imaging system, the results show that the larger the comprehensive resolution of the LWIR imaging system, the smaller the ratio of the target recognition range of the two systems.

The comprehensive resolution of MER-20-20GM is smaller than that of Aca640-90gm. According to Eq. (19), the predictive ratio of target recognition range of MER-20-20GM to that of Gobi-640-Gige is larger than the predictive ratio of the target recognition range of Aca640-90gm to that of Gobi-640-Gige. The same goes for the experimental results. X8500sc-SLS also has the same phenomenon as Gobi-640-Gige. For the same LWIR imaging system, the results show that the larger the comprehensive resolution of visible imaging system, the larger the ratio of the target recognition range of the two systems.

6 Conclusions

Without considering the factors such as the signal-to-noise ratio of the imaging system, the atmospheric spectral transmittance, and the transmittance of the optical system, the performance of four typical common-aperture VaLWIRIS was analyzed by using the comprehensive resolution.

Under the conditions of wavelength, detector size, focal length, and clear aperture given in this study, the visible imaging system performance is generally detector-limited, while the LWIR imaging system performance may be detector-limited, optics-limited, or transitional. The research results show that when the comprehensive resolution of the visible imaging system increases, the target recognition ranges of the visible imaging system and the LWIR imaging system increase, as well as the ratio of the target recognition ranges of the two systems increases.

Funding information: The authors state no funding involved.

Author contributions: All authors have accepted responsibility for the entire content of this manuscript and approved its submission.

Conflict of interest: The authors state no conflict of interest.

References

[1] Cheng ZF, Liu FH, Xun XC. Opto-mechanical design and analysis of dual-band sharing aperture imaging system. Infrared Laser Eng. 2015;44(11):3366–72.

[2] Lin Q, Jin WQ, Guo H, Zhang YZ, Li MZ. Confocal-window telescope objective design in visible and LWIR. Acta Optica Sinica. 2012;32(9):09220051–09220055. doi: 10.3788/AOS201232.0922005.
[3] Ezzat MA, El-Bary AA. Magneto-thermoelectric viscoelastic materials with memory dependent derivative involving two-temperature. Int J Appl Electromagn Mech. 2016;50:549–67. doi: 10.3233/JAE-150131.
[4] Lotfy K, Hassan W, El-Bary AA, Kadry MA. Response of electromagnetic and Thomson effect of semiconductor medium due to laser pulses and thermal memories during photothermal excitation. Results Phys. 2020;16:1–8.
[5] Sun T, Zhu HY, Yang ZJ, Zhang XZ, Yang HM. Design of dual-band common-aperture camera optical system. J Appl Opt. 2017;38(3):348–1. doi: 10.5678/JAO2017380301002.
[6] Wang CC, Zhou GY, Pang ZH, Li RC. Design of large field for visible/infrared integrated optical system. Infrared Laser Eng. 2016;45(10):164–9. doi: 10.3788/IRLA201645.1018003.
[7] Cui EK. The design of visible and infrared multi-band optical system. Master's Thesis. Changchun (JL): Chinese Academy of Sciences; 2014.
[8] Richard V. Night vision integrated performance model: impact of a recent change on the model's predictive accuracy. Opt Exp. 2016;24(21):23654–66.
[9] Jonathan GH, Brian PT, John JG, George N. Analysis and modeling of observer performance while using an infrared imaging system. Opt Eng. 2020;59(3):0331061–03310614. doi: 10.1117/1.OE.59.3.033106.
[10] Gerald CH. Imaging system performance based upon Fλ/d. Opt Eng. 2007;46(10):1032041–1032048. doi: 10.1117/1.2790066.
[11] Ronald D, Glenn G, Steve B, Gerald H, Orges F. Simple target acquisition model based on Fλ/d. Opt Eng. 2021;60(2):0231041–02310412. doi: 10.1117/1.OE.60.2.023104.
[12] Robert DF. Image quality and λFN/ρ for remote sensing systems. Opt Eng. 1999;38(7):1229–40.
[13] Robert DF. Modeling the imaging chain of digital cameras. 1st edn. WA: SPIE Press; 2012.